

Magnetic structures of quaternary intermetallic borocarbides

$R\text{Co}_2\text{B}_2\text{C}$ ($R=\text{Dy, Ho, Er}$).

M. ElMassalami, R. Moreno

*Instituto de Fisica, Universidade Federal do Rio de Janeiro,
Caixa Postal 68528, 21945-970 Rio de Janeiro, Brazil*

H. Takeya

*National Institute for Materials Science,
1-2-1 Sengen, Tsukuba, Ibaraki 305-0047, Japan*

B. Ouladdiaf

Institut Laue-Langevin, B.P.156 ,38042 Grenoble Cedex 9, France

J. W. Lynn

*NIST Center for Neutron Research,
National Institute of Standards and Technology, Gaithersburg, MD 20899-6102*

R. S. Freitas

*Instituto de Física., Universidade de São Paulo,
Rua do Matão 187 Travessa R, Cidade Universitária,
05315-970 Sao Paulo, SP , Brasil*

(Dated: November 4, 2018)

Abstract

The magnetic structures of the title compounds have been studied by neutron diffraction. In contrast to the isomorphous RNi_2B_2C compounds wherein a variety of exotic incommensurate modulated structures has been observed, the magnetic structure of $ErCo_2B_2C$ is found to be collinear antiferromagnet with $k=(\frac{1}{2}, 0, \frac{1}{2})$ while that of $HoCo_2B_2C$ and $DyCo_2B_2C$ are observed to be simple ferromagnets. For all studied compounds, the moments are found to be confined within the basal plane and their magnitudes are in good agreement with the values obtained from the low-temperature isothermal magnetization measurements. The absence of modulated magnetic structures in the RCO_2B_2C series (for $ErCo_2B_2C$, verified down to 50 mK) is attributed to the quenching of the Fermi surface nesting features.

I. INTRODUCTION

One of the most striking features of the magnetism of the $R\text{Ni}_2\text{B}_2\text{C}$ series is the manifestation of a variety of incommensurate modulated antiferromagnetic-like modes, some of which coexist with a superconducting ground state.^{1,2,3} There are three different types of modulations that have been observed: $\vec{k}_1 \simeq (0.55, 0, 0)$ as in $R = \text{Er, Ho}$ [$4.5 < T < 6.5$ K], Tb , and Gd ; $\vec{k}_2 \simeq (0.093, 0.093, 0)$ as in $R = \text{Tm}$; and $\vec{k}_3 \simeq (0, 0, 0.91)$ as in $R = \text{Ho}$ [$5 < T < 8$ K]. In addition, there are two commensurate antiferromagnetic (AFM) structures having $\vec{k}_4 = (0, 0, 1)$ as in $R = \text{Ho, Dy, Pr}$ and $\vec{k}_5 = (0.5, 0, 0.5)$ as in $R = \text{Nd}$. For the case of $R = \text{Ho}$, the \vec{k}_1 , \vec{k}_3 , and \vec{k}_4 modes coexist within a narrow range of temperature.² The manifestation of such a variety of wave vectors is not uncommon in intermetallic magnets wherein the magnetic couplings are mediated by the indirect Ruderman-Kittel-Kasuya-Yosida (RKKY) interactions:⁴ indeed for the particular case of $R\text{Ni}_2\text{B}_2\text{C}$, the presence of these RKKY interactions is evidenced as a de Gennes scaling of both the superconducting and magnetic transition temperatures.^{1,3}

As is generally the case, the type of the magnetic structure for the rare-earth moments in $R\text{Ni}_2\text{B}_2\text{C}$ is determined by the competition between these RKKY interactions, the crystalline electric field (CEF) forces, and the classic dipolar interactions.^{5,6,7} The RKKY interactions (and thus the magnetic structure) depend partially on the spatial separation of the R^{3+} ions as well as on the electronic band structure of these borocarbides. The importance of the latter is highlighted by the finding that the \vec{k}_1 mode is related to the electronic nesting features that give rise to a peak in the generalized susceptibility.⁸

It is worth mentioning that the manifestation of a variety of wave vectors in the members of the $RT_2\text{B}_2\text{C}$ family is not forbidden by group theory arguments.^{9,10,11} In fact, for these tetragonal borocarbides ($I4/mmm$) where the magnetic moments reside at the Wyckoff site $2a$, Wills *et al.*⁹ showed that there are fifteen possible wave vectors, each (or a superposition) of them can be used to describe a distinct magnetic structure (see Table 3 of Ref.⁹). As mentioned above, the stabilization of a specific mode depends critically on the energy balance among the CEF, dipolar, and exchange interactions. It is interesting to note that this representational analysis predicts the possibility of a ferromagnetic (FM) mode in this $RT_2\text{B}_2\text{C}$ family: such a mode has not been observed in $R\text{Ni}_2\text{B}_2\text{C}$ but, as shown in previous reports^{12,13} as well as in this work, a FM mode is manifested in a number of $R\text{Co}_2\text{B}_2\text{C}$

compounds.

The electronic band structures of the RT_2B_2C ($T=\text{Ni, Co}$) family of compounds are very similar.¹⁴ In addition, both series have almost the same Sommerfeld specific-heat coefficients. Furthermore, each isomorphous pair has almost equal lattice parameters and very much similar R^{3+} single-ion crystalline-electric field properties.¹⁵ Then it is expected that the multi wave-vectors character to be manifested also in the isomorphous RCO_2B_2C series. Contrary to this expectation, the reported magnetic structures of RCO_2B_2C ($R=\text{Tb}$ [Ref.¹³], Tm [Ref.¹²]) are found to be ferromagnetic: in distinct contrast to the modulated spin configuration of the Ni-based isomorphs. As this work shows, the magnetic structures of RCO_2B_2C ($R = \text{Dy, Ho, Er}$) are also ferromagnetic and different from their Ni-based isomorphs.

The difference in the magnetic structure of these isomorphous RT_2B_2C ($T=\text{Ni, Co}$) series is attributed to the following:^{12,13} electronic band structure calculations^{14,16,17,18} demonstrated that the density of states at the Fermi level, $N(E_F)$, of both series receives appreciable contribution from the $3d$ orbitals of the transition-metal atoms. As that the electronic properties of the RT_2B_2C family can be reasonably well described in terms of the rigid band model, the substitution of Co atoms (which has a lower number of the $3d$ electrons) induces a downward shift in E_F but with a new $N(E_F)$ which is almost equal to that of RNi_2B_2C [compare Figs. 1 and 4 of Ref.¹⁴]. Such a shift entails a different generalized susceptibilities and thus a different character of the magnetic ground state. In particular, the absence of modulated states in RCO_2B_2C is taken to be a strong indication that the characteristic nesting features at, say, \vec{k}_1 must have been quenched.

II. EXPERIMENT

99.5% ^{11}B enriched polycrystals of RCO_2B_2C were prepared by conventional arc-melt method. Powder neutron-diffraction measurements on as-prepared samples were carried out at the Institut Laue-Langevin in Grenoble, France ($\lambda = 2.359 \text{ \AA}$, $0.48 \leq T \leq 4.5 \text{ K}$) and the National Institute of Standards and Technology, USA (BT-9 triple-axis instrument with a pyrolytic graphite monochromator and filter, $\lambda = 2.359 \text{ \AA}$, $0.05 \leq T \leq 8.0 \text{ K}$, and BT-1 high resolution powder diffractometer with $\lambda = 2.0787 \text{ \AA}$). Due to the experimental difficulties, the neutron diffractograms within the mK range were measured only for $\text{ErCo}_2\text{B}_2\text{C}$ (§ III.A).

Similarly, detailed temperature-dependent diffractograms were collected only for $\text{HoCo}_2\text{B}_2\text{C}$ (§ III.B).

Powder Rietveld refinements of both crystallographic and magnetic structures were carried out using the FULLPROF package of Rodriguez-Carvajal (L. L. B.).

Magnetization $M(T, H)$ measurements (§ III.B-C) were conducted in a vibrating-sample magnetometer which was operated within the range $[0.5 < T < 30 \text{ K}, H < 17 \text{ T}]$.

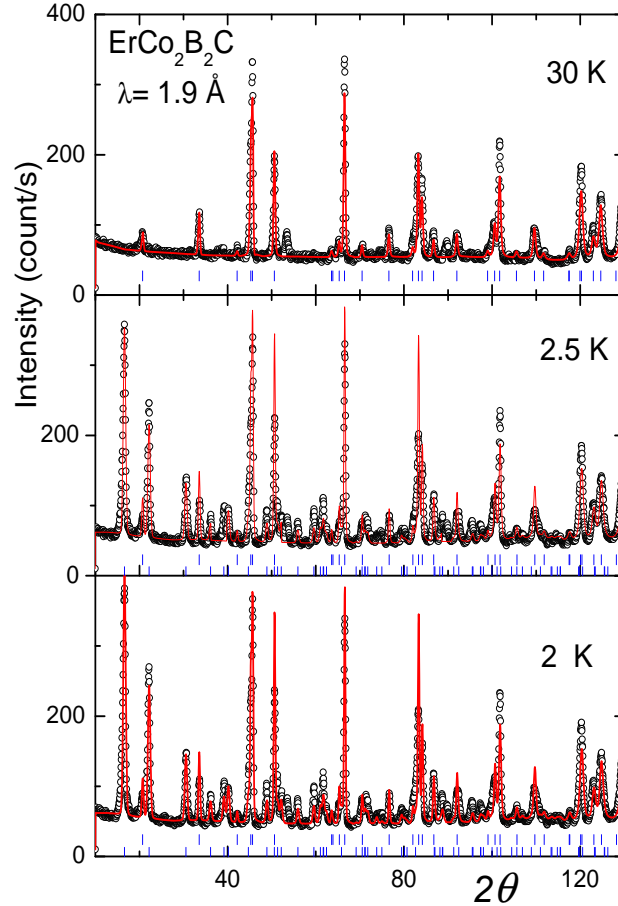


FIG. 1: (Color online) Representative neutron diffractograms of $\text{ErCo}_2\text{B}_2\text{C}$ measured at 2 K (low panel), 2.5 K (middle panel), and 30 K (top panel). Symbols, solid line, and short vertical bars represent, respectively, measured intensities, calculated intensities based on Rietveld-refinement, and positions of the Bragg reflections (see text).

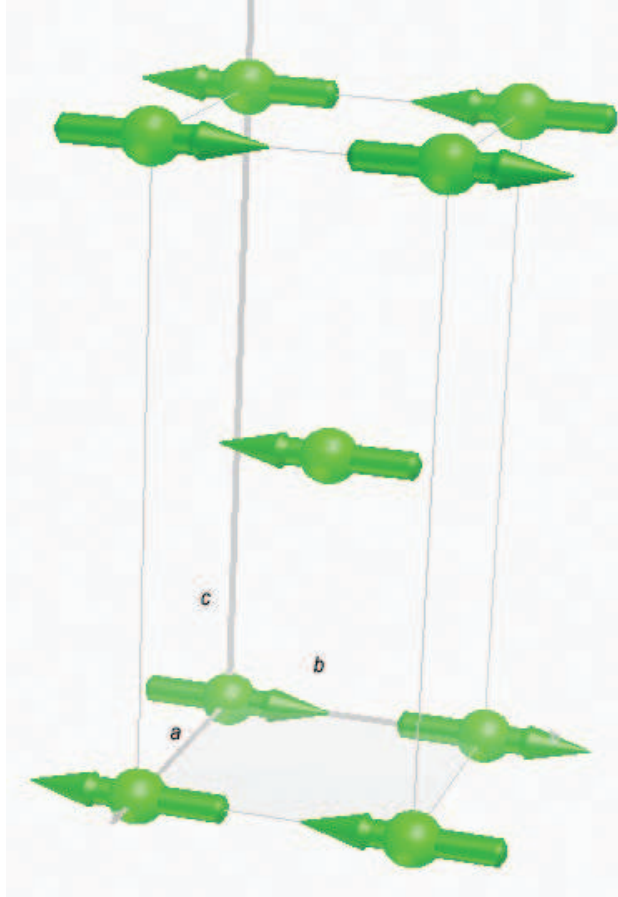


FIG. 2: The commensurate, collinear, antiferromagnetic structure of $\text{ErCo}_2\text{B}_2\text{C}$. The moments are coupled antiferromagnetically along both the a and c axis and ferromagnetically along the b axis.

III. RESULTS

A. $\text{ErCo}_2\text{B}_2\text{C}$

Based on earlier zero-field ac susceptibility and specific heat results,¹⁵ the magnetic order of $\text{ErCo}_2\text{B}_2\text{C}$ sets-in at $T_N = 4.0(1)$ K. Indeed, below T_N the diffractograms of $\text{ErCo}_2\text{B}_2\text{C}$ (Fig. 1) show a number of additional intense Bragg peaks which can be indexed on the basis of the magnetic structure given in Fig. 2: a commensurate, collinear, antiferromagnetic structure with the moments being coupled antiferromagnetically along both a and c axes and ferromagnetically along the b axis; i.e. $k=(\frac{1}{2} \ 0 \ \frac{1}{2})$. This AFM character of the ordered state is manifested also in the magnetization isotherm of Fig. 3.

Based on the refinement of the powder diffractograms (Fig. 1), the Er^{3+} moments are

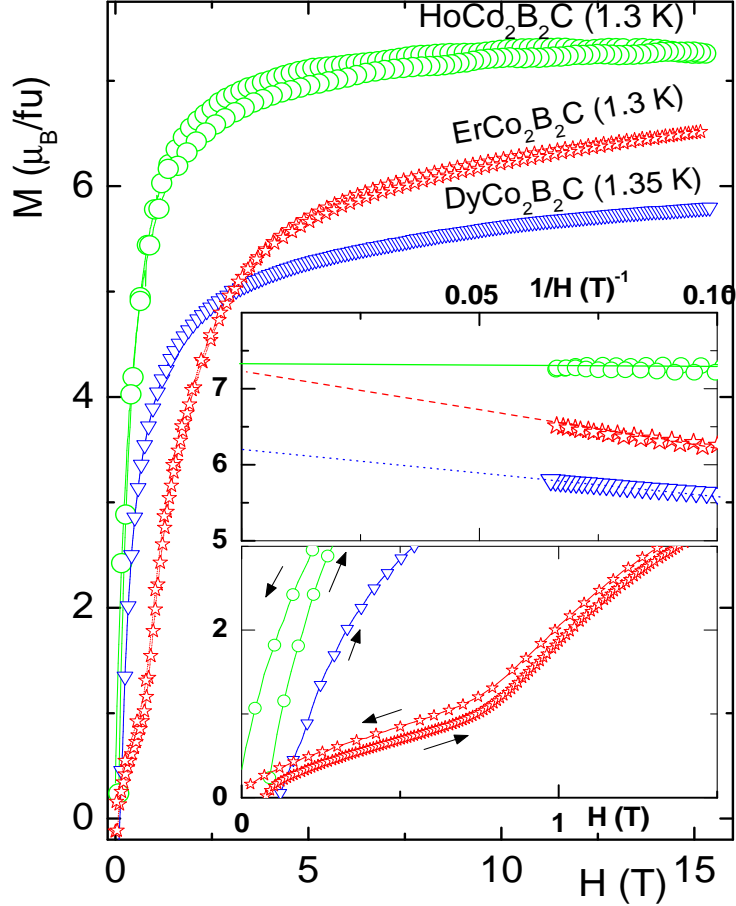


FIG. 3: (Color online) Magnetization isotherms of $R\text{Co}_2\text{B}_2\text{C}$ ($R=\text{Dy}, \text{Ho}, \text{Er}$) measured at the indicated temperatures. The lower inset shows an expansion of the low-field region of the forced magnetization: while $M(T, H)$ of $R=\text{Dy}, \text{Ho}$ is typical of a forced FM state, that of $R=\text{Er}$ is characteristic of a field-induced spin-flop anomaly of an AFM structure. The upper inset demonstrates the saturated magnetization when $H \rightarrow \infty$ ($\frac{1}{H} \rightarrow 0$): for $R=\text{Er}$ and Dy , no saturation is attained even for a field of 15 T. The extrapolated values when $\frac{1}{H} \rightarrow 0$ are shown in Table I. Similar high-field magnetization features were observed in $\text{TbCo}_2\text{B}_2\text{C}$ (see Fig. 2 of Ref.¹³) and $\text{TmCo}_2\text{B}_2\text{C}$ (see Fig. 6 of Ref.¹²).

found to be confined within the basal plane and reach $6.8(2) \mu_B$ at 2.0 K. This value is in excellent agreement with the saturated moment $7.0(2) \mu_B$ obtained from the isothermal magnetization measured at $1.40(5)$ K (Fig. 3). Moreover, it compares favorably with the value reported for $\text{ErNi}_2\text{B}_2\text{C}$ ($\mu = 7.2 \pm 0.1 \mu_B$),² suggesting a similarity in their single-ion properties. However, there are important differences between these two isomorphs: the

Co-based isomorph does not superconduct and does not have an incommensurate magnetic structure, instead ordering into a collinear AFM structure at a critical temperature that is 40% lower than that of the Ni-based isomorph.

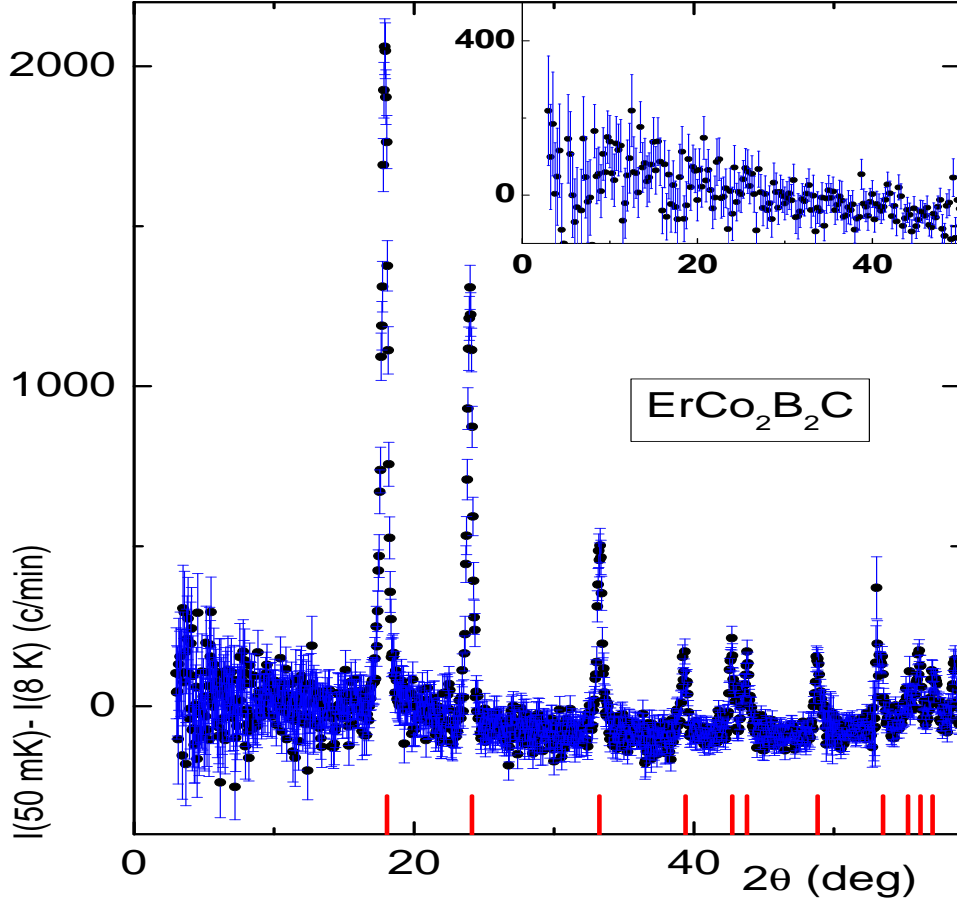


FIG. 4: (Color online) Low-temperature magnetic diffractogram of $\text{ErCo}_2\text{B}_2\text{C}$ obtained after subtracting the nuclear contributions (diffractogram at 8 K) from the one at 50 mK; the solid vertical bars index the magnetic pattern. The inset shows the difference pattern obtained after subtracting the diffractogram at 700 mK from that of 50 mK: evidently there is no change in the magnetic structure (see text). Uncertainties where indicated in the manuscript are statistical in nature and represent one standard deviation.

It was reported earlier that both the specific heat and *ac* susceptibility curves of an $\text{ErCo}_2\text{B}_2\text{C}$ sample exhibit a magnetic anomaly at $T_M = 0.37(2)$ K.¹⁵ For the purpose of investigating the origin of the reported anomaly, we collected neutron diffractograms at various temperatures: 50 mK (well below T_M), 700 mK (just above T_M but well below T_N),

and 8 K (above T_N). As can be seen in Fig. 4, there are no additional magnetic peaks (nor any other features) that can be associated with this anomaly. In fact the inset of Fig. 4 indicates that the magnetic patterns at 700 mK and 50 mK are identical. As there are no change in the diffractograms when the temperature is cooled through the reported T_M , it is concluded that the reported anomalous transition at T_M may correspond to an ordered moment that is too small to be detected in powder diffraction, or it does not correspond to a new long-range ordered state. We also cannot rule out that it is a sample dependent effect, which would imply that it is not intrinsic to the Er-sublattice.

B. $\text{HoCo}_2\text{B}_2\text{C}$

The diffractograms of $\text{HoCo}_2\text{B}_2\text{C}$ (Fig. 5) show that there are no additional satellite peaks when the sample is cooled to below $T_C = 5.4(2)$ K; instead, there is a considerable enhancement in the intensities of the fundamental Bragg peaks. The resulting magnetic pattern is easily indexed on the basis of a FM unit cell which is of the same dimension as the crystalline one. The Rietveld analysis (see Fig. 6) confirms the conclusions drawn from the magnetic indexing: a FM structure with the moments lying within the basal plane. The thermal evolution of the Ho^{3+} moments (Fig. 7) shows a tendency towards saturation at an ordered value of the moment of $7.2(2) \mu_B$. This is in excellent agreement with the saturation moment of $7.3(1) \mu_B$ obtained from the isothermal magnetization measurement (see Fig.3). Furthermore, Fig 7 indicates that the intensity monotonically decreases as T_C is being approached from below, and at higher T decreases almost linearly and becomes zero at 7.6 K. The presence of magnetic intensity well above T_C (attributed to short range order) has already been observed in the specific heat and susceptibility of $\text{HoCo}_2\text{B}_2\text{C}$.¹⁵ Similar short-range features were observed in the neutron diffraction studies on the $\text{HoNi}_2\text{B}_2\text{C}$ isomorph.²

In stark contrast with the exotic features of the low-temperature magnetic phase diagram of $\text{HoNi}_2\text{B}_2\text{C}$,^{1,3} the above results demonstrate that $\text{HoCo}_2\text{B}_2\text{C}$ orders into a simple FM state and that within the studied temperature range [$1.4 \text{ K} < T < T_C$] there are no manifestations of additional zero-field order-to-order magnetic transformations. This corrects our earlier report of a magnetic transition at $T_m=1.5$ K.¹⁵ Even though in this work we were not able to collect diffractograms below 1.4 K, considering the similarity with $\text{ErCo}_2\text{B}_2\text{C}$ (see § IV.C) and $\text{TbCo}_2\text{B}_2\text{C}$ (Ref.¹³), no order-to-order transitions or modifications in the magnetic

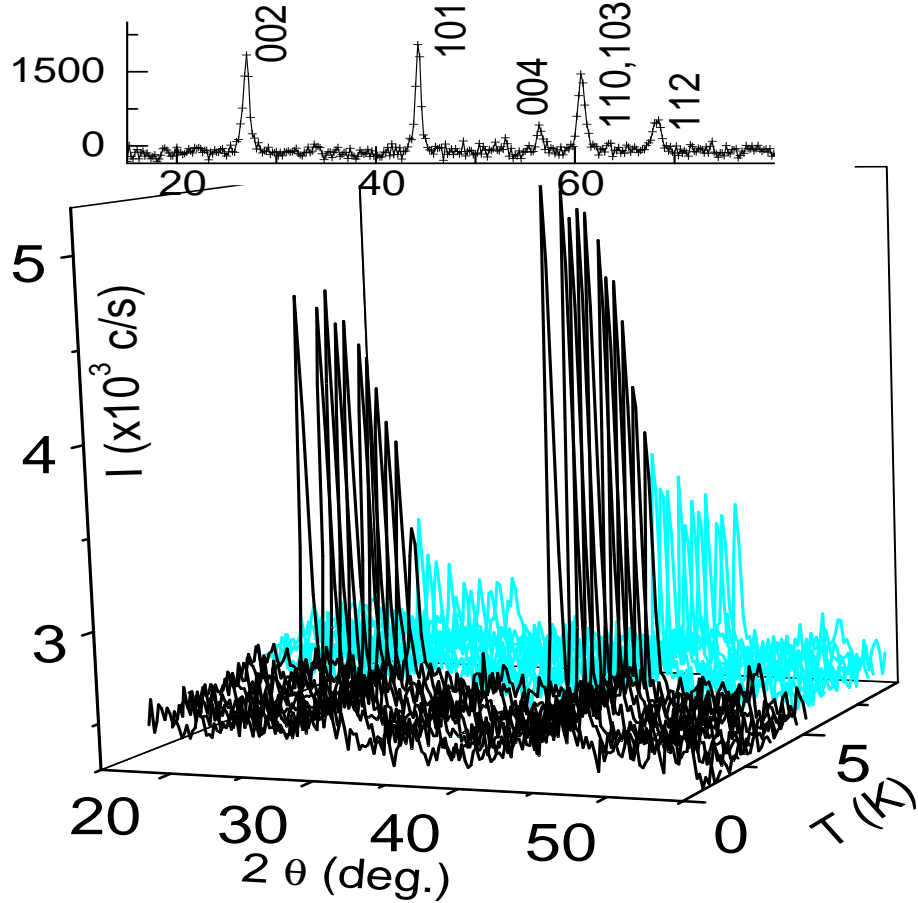


FIG. 5: (Color online) Lower panel: three dimensional plot of representative powder diffractograms of $\text{HoCo}_2\text{B}_2\text{C}$. The intensities are measured over a wide range of scattering angle (for clarity, here shown only up to 55°) and at various temperatures. The enhancement of the intensities at the positions of the nuclear Bragg peaks is clearly manifested below T_C . The fact that there are no additional magnetic peaks and that the Ho site is at $4a$ site indicates that the magnetic arrangement must be due to an onset of ferromagnetism (see text). This is confirmed in the upper panel which shows the difference plot of $I(1.5\text{K})-I(10\text{K})$ together with the Bragg peaks identifications.

structure of Ho sublattice are expected to occur.

C. $\text{DyCo}_2\text{B}_2\text{C}$

Figure 8 shows the thermal evolution of the diffraction pattern of $\text{DyCo}_2\text{B}_2\text{C}$ when cooled through the magnetic transition temperature [$T_C = 8.0(2)\text{K}$].¹⁵ On subtracting the param-

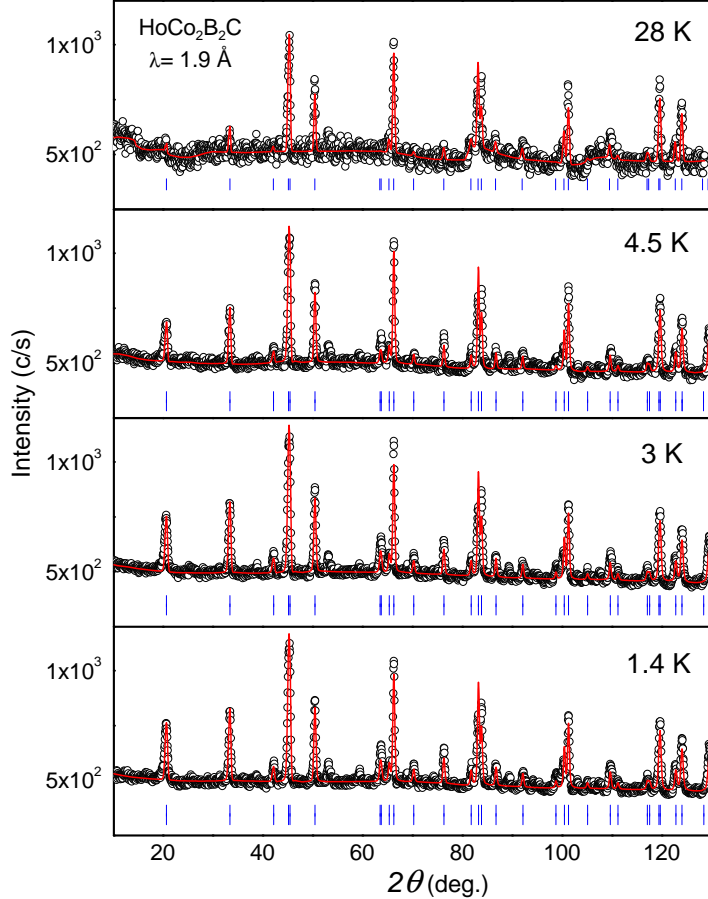


FIG. 6: (Color online) Rietveld refinement of representative powder diffractograms of $\text{HoCo}_2\text{B}_2\text{C}$. Symbols, solid line, and short vertical bars represent, respectively, measured intensities, calculated intensities based on Rietveld-refinement, and positions of the Bragg reflections. The total contribution is composed of nuclear peaks ($I4/mmm$) and the FM order of the Ho subsystem (see text).

agnetic diffractogram at 10 K from the one at 1.4 K, we obtained the magnetic diffraction pattern shown in the inset of Fig. 8. This pattern is indexed on the basis of a FM cell having the same cell dimensions as those of the crystalline one. We attempted to refine the neutron-diffractogram (Fig. 8), but due to the relatively high neutron absorption of Dy, the statistics are not adequate to allow a reliable determination of the ordered moment. Nevertheless, it is inferred that the moments lie within the ab -plane and its value at least exceeds $4.6 \mu_B$. To get a better evaluation of the saturated moment, we resorted to the magnetization isotherm. Fig. 3 indicates that the saturated moment at 1.35 K is $6.2(1) \mu_B$;

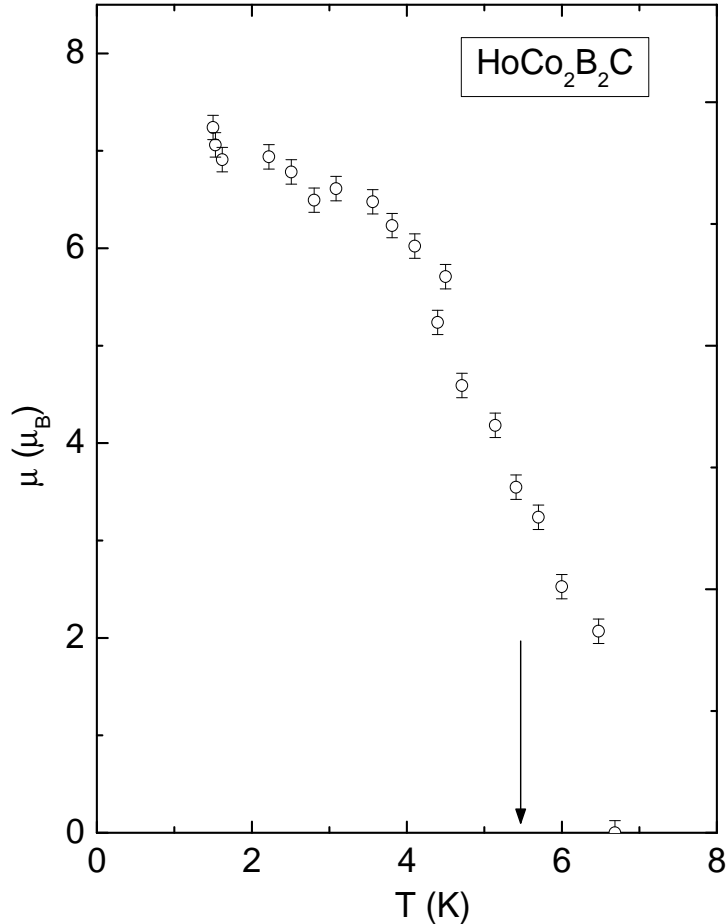


FIG. 7: Thermal evolution of the ordered magnetic moment for $\text{HoCo}_2\text{B}_2\text{C}$ as obtained from the neutron diffraction refinements of Fig. 6.

this value is 29% lower than the value reported for the $\text{DyNi}_2\text{B}_2\text{C}$ isomorph.

IV. DISCUSSION AND CONCLUSION

As mentioned above, the crystalline electric field environment around the R^{3+} site in the RT_2B_2C family is expected to be the same as the one observed in the isomorphous $R\text{Ni}_2B_2C$ systems. Consequently the single-ion properties of R^{3+} (such as the ordered moment, direction, and magnetoelastic properties) should be similar. In particular, the magnetic easy axes in the sequence of compounds $\text{Er}T_2B_2C$, $\text{Ho}T_2B_2C$, and $\text{Dy}T_2B_2C$ ($T = \text{Co}, \text{Ni}$) should be similar (see Table I). This working assumption is particularly helpful since the zero-field powder neutron diffraction technique is not able to identify the easy axis, even though it

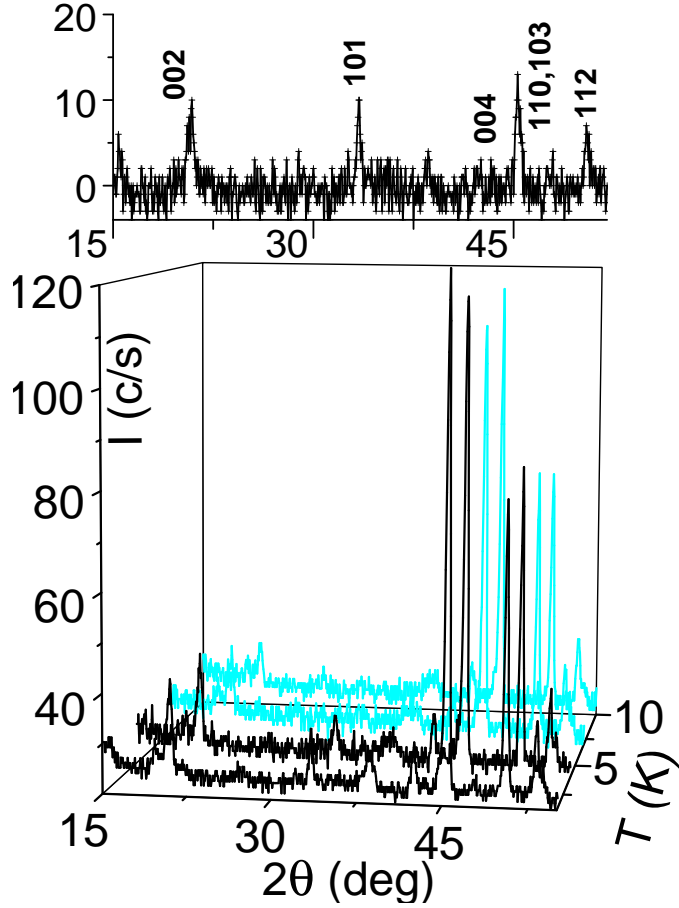


FIG. 8: (Color online) Lower panel: representative diffractograms of $\text{DyCo}_2\text{B}_2\text{C}$ measured at 1.4, 4, 7, and 10 K. The upper panel shows the difference plot (after subtracting of the pattern at 10 K from the one at 1.4 K): the pattern is indexed based on a ferromagnetic structure.

successfully identified the easy character of the ab -plane. Then based on this similarity of the CEF properties, the easy axis of both $R = \text{Ho}, \text{Dy}$ is taken to be $(1, 1, 0)$ while that of $R = \text{Er}$ is $(1, 0, 0)$ axis. It is reassuring that these arguments proved to be valid for the case of $\text{TbCo}_2\text{B}_2\text{C}$ (see Table I and Ref.¹³).

The observation that none of the studied $R\text{Co}_2\text{B}_2\text{C}$ compounds exhibit an incommensurate modulated state is argued to be an indication that the Fermi surface nesting features are quenched.¹³ Another striking difference between the isomorphous $RT_2\text{B}_2\text{C}$ ($R = \text{Dy}, \text{Ho}$) compounds is shown in Fig. 3: the absence of metamagnetic field-induced transitions in the magnetization isotherms. This feature is most evident in the magnetization isotherms of single-crystal $\text{TbCo}_2\text{B}_2\text{C}$ (see Fig. 2 of Ref.¹³). These two observations highlight the

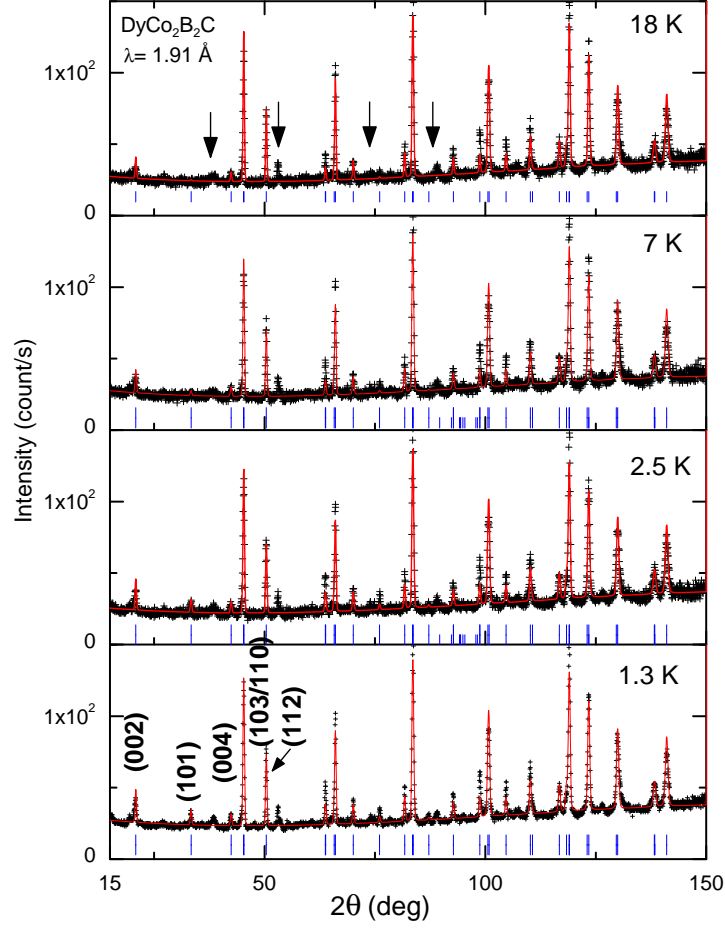


FIG. 9: Refinements of representative diffractograms of $\text{DyCo}_2\text{B}_2\text{C}$. Except for the weak impurity peaks (denoted by short vertical arrows), all peaks (symbol) are fit (solid lines) based on the following crystalline and magnetic structures: a tetragonal unit cell ($I4/mmm$ with lattice parameters as given in Table I) and a FM unit cell (Bragg peaks shown as short vertical bars) having the same dimensions.

delicate balance of the exchange, crystalline, and dipolar interactions in $R\text{Ni}_2\text{B}_2\text{C}$ for establishing their exotic magnetic phase diagrams: it is recalled that $\text{GdNi}_2\text{B}_2\text{C}$ (wherein there are exchange and dipolar forces but no CEF interaction) does manifest a modulated state but no cascade of field-induced metamagnetic transformations. On the other hand, none of the studied $R\text{Co}_2\text{B}_2\text{C}$ ($R=\text{Dy}, \text{Ho}$) compounds exhibit a modulated state or a cascade of metamagnetic transformations even though these compounds do possess exchange, CEF and dipolar forces that are similar to those of the Ni-based isomorphs.

The FM structure of $R\text{Co}_2\text{B}_2\text{C}$ ($R= \text{Tm}$ [Ref.¹²], $\text{Ho}, \text{Dy}, \text{Tb}$ [Ref.¹³]) is expected to

TABLE I: Some structural and magnetic parameters of the isomorphous RNi_2B_2C and RCO_2B_2C series ($R = Tm, Er, Ho, Dy, Tb$). The room-temperature cell dimensions of RNi_2B_2C (RCO_2B_2C) are determined from neutron¹⁹ (X-ray^{12,15}) diffraction. The magnetic properties of RNi_2B_2C are taken from Ref.^{19,20} while those of $TbCo_2B_2C$ and $TmCo_2B_2C$ are taken, respectively, from Ref.¹³ and Ref.¹². The symbols have their usual meanings. $|\vec{\mu}|$ refers to the value obtained from the neutron diffraction analysis.

R	Tm		Er		Ho		Dy		Tb	
M	Co	Ni	Co	Ni	Co	Ni	Co	Ni	Co	Ni
a (Å)	3.473	3.4866	3.4844	3.5019	3.4997	3.5177	3.5099	3.53420	3.5246	3.5536
c (Å)	10.647	10.607	10.5902	10.5580	10.54465	10.5278	10.5268	10.4878	10.5176	10.4352
T_{crit} (K)	0.8	1.53	4.0	6.8	5.4	5.0	8.0	10.6	6.3	15.0
Mode	FM	TSW	AFM	TSW	FM	AF	FM	AF	FM	LSW
k	(0,0,0)	(0.093,0.093,0)	($\frac{1}{2}, 0, \frac{1}{2}$)	(0.553,0,0)	(0,0,0)	(0,0,1)	(0,0,0)	(0,0,1)	(0,0,0)	(0.555,0,0)
$ \vec{\mu} $	~ 1	3.8	6.8(2)	7.2	7.2(2)	8.6	>4.6	8.5	7.6	7.8
easy axis	(0,0,1)	(0,0,1)	(0,1,0)	(0,1,0)	(1,1,0)	(1,1,0)	(1,1,0)	(1,1,0)	(1,0,0)	(1,0,0)

generate a large internal molecular field at the Co-sublattice. Then if this internal field exceeds a certain critical value, the Co-sublattice could be spontaneously polarized.^{21,22,23,24} We were particularly interested in this prospect of Co-sublattice polarization since this scenario was thought to support our earlier report of a second metamagnetic transformation (T_M boundary) in the magnetic phase diagram of RCO_2B_2C .¹⁵ It happened that the neutron diffractograms of $R=Dy, Ho, Er$ compounds as well those of $TbCo_2B_2C$ [Ref.¹³] and $TmCo_2B_2C$ [Ref.¹²] do not show any intrinsic transformation. Furthermore, this T_M transition is not always manifested in the recent thermodynamical measurements on $TbCo_2B_2C$.¹³ Consequently, it is concluded that there is no spontaneous polarization of the Co-sublattice: if there is any it must be sample dependent.

In conclusion, this work showed that the ground states as well as the magnetic phase diagrams of the studied RCO_2B_2C compounds are distinctly different from those of their Ni-based isomorphs. These findings should certainly contribute to our understanding of the magnetism, superconductivity and their interplay in the borocarbides series.

Acknowledgments

We acknowledge the partial financial support from the Brazilian agencies CNPq (485058/2006-5), Faperj (E-26/171.343/2005), and FAPESP (2008/00457-2).

-
- ¹ K.-H. Müller and V. N. Narozhnyi, Rep. Prog. Phys. **64**, 943 (2001).
 - ² J. W. Lynn, S. Skanthakumar, Q. Huang, S. K. Sinha, Z. Hossain, L. C. Gupta, R. Nagarajan, and C. Godart, Phys. Rev. B **55**, 6584 (1997).
 - ³ P. C. Canfield, P. L. Gammel, and D. J. Bishop, Phys. Today **51**, 40 (1998).
 - ⁴ B. Coqblin, *The Electronic Structure of Rare-Earth Metals and Alloys: The Magnetic Heavy Rare-Earth* (Academic Press, New York, 1977).
 - ⁵ V. A. Kalatsky and V. L. Pokrovsky, Phys. Rev. B **57**, 5485 (1998).
 - ⁶ A. Amici and P. Thalmeier, Phys. Rev. B **57**, 10 684 (1998).
 - ⁷ J. Jensen, Phys. Rev. B **65**, 140514(R) (2002).
 - ⁸ J. Y. Rhee, X. Wang, and B. N. Harmon, Phys. Rev. B **51**, 15 585 (1995).
 - ⁹ A. S. Wills, C. Detlefs, and P. C. Canfield, Phil. Mag. **83**, 1227 (2003).
 - ¹⁰ R. Ballou and B. Ouladdiaf, in *Neutron Scattering from Magnetic Materials*, edited by T. Chatterji (Elsevier, 2006), p. xxx.
 - ¹¹ Y. A. Izyumov, V. E. Naish, and R. P. Ozerov, *Neutron Diffraction of Magnetic Materials* (Consultants Bureau, New York, 1991).
 - ¹² M. ElMassalami, R. E. Rapp, F. A. B. Chaves, R. Moreno, H. Takeya, B. Ouladdiaf, J. W. Lynn, Q. Huang, R. S. Freitas, and N. F. Oliveria Jr., J. Phys.: Condens. Matter **21**, in press (2009).
 - ¹³ M. ElMassalami, R. Moreno, R. M. Saeed, F. A. Chaves, H. Takeya, B. Ouladdiaf, and M. Amara, J. Phys: Condens Matter **21** (2008), (submitted).
 - ¹⁴ R. Coehoorn, Physica C **228**, 331 (1994).
 - ¹⁵ M. ElMassalami, M. S. DaCosta, R. E. Rapp, and F. A. B. Chaves, Phys. Rev. B **62**, 8942 (2000).
 - ¹⁶ W. E. Pickett and D. J. Singh, Phys. Rev. Lett **72**, 3702 (1994).
 - ¹⁷ L. F. Matthias, Phys. Rev. B **49**, 13279 (1994).

- ¹⁸ J. I. Lee and et al, Phys. Rev. B **50**, 4030 (1994).
- ¹⁹ J. W. Lynn, Q. Huang, S. K. Sinha, Z. Hossain, L. C. Gupta, R. Nagarajan, and C. Godart, J. Appl. Phys. **79**, 5857 (1996).
- ²⁰ L. J. Chang, C. V. Tomy, D. M. Paul, and C. Ritter, Phys. Rev. B **54**, 9031 (1996).
- ²¹ D. Bloch and R. Lemaire, Phys. Rev. B **2**, 2648 (1970).
- ²² D. Bloch, D. M. Edwards, M. Shimizu, and J. Voiron, J. Phys. F: Metal Phys. **5**, 1217 (1975).
- ²³ M. Cyrot and M. Lavagna, J. Phys. (Paris) **40**, 763 (1979).
- ²⁴ M. Cyrot, D. Gignoux, F. Givourd, and M. Lavagna, J. Phys. (Paris) **40**, C5 (1979).